

Hassan Kahil

Introduction to the dynamic theory of the (H⁺, e⁻) couple insertion in γ -MnO₂

Received: 11 November 1998 / Accepted: 25 March 1999

Abstract This paper presents a phenomenological theory of coupled H⁺ and e⁻ diffusion in γ/ε -MnO₂. A set of five dynamic regimes governs the (H⁺, e⁻) insertion during the entire reduction ($0.08 < r < 1$) of the dioxide. It is imposed by a global balance of several physical quantities which depend on the reduction level r . The principal potential factor for the diffusion in a given direction is the difference between the components, along this direction, of the self velocities V_{e^-} and V_{H^+} . The longitudinal component E_{ld} of the internal electric field vector E_d plays, with respect to electrons and protons, the velocity regulator role. The transversal component E_{td} allows some homogenisation of (H⁺, e⁻) concentration during the first half of the reaction and trapping of electrons in the second half. Towards $r \approx 0.50$, V_{e^-} and V_{H^+} are equal, the internal electric field reverses its orientation after taking a null value and the first Mn³⁺ ions appear. This introduction to the dynamic theory of γ/ε -MnO₂ is a new finding and can interpret most of its physical/chemical properties, especially the behaviour change around $r \approx 0.50$.

Key words Manganese dioxide · Dynamic theory · (H⁺, e⁻) insertion

$\langle v \rangle, \langle v' \rangle$	Electric and thermodynamic drift velocity vectors
F'	Thermodynamic transport force
a_i	Activity of the species i
f_i	Activity coefficient of the species i
ε	Thermodynamic potential
E_d	Internal electric field vector
S_r	Reactive surface
e	Elementary electric charge
\tilde{D}	Ambipolar diffusion tensor
\underline{D}	Mean value of the diffusion tensor terms
r	γ/ε -MnO ₂ reduction degree
x	Mn ⁴⁺ vacancy fraction
y	Mn ³⁺ fraction
ρ	γ -MnO ₂ mean grain radius
S	Solvent
P	Pair concentration
$(C - P)$	Unpaired e ⁻ or H ⁺ concentration
C'	MnO ₆ ⁸⁻ or O ₆ ¹²⁻ concentration
EMD-ICS	Electrolytic manganese dioxide-international common sample
Ω	Dynamic equilibrium constant
\tilde{V}	Self velocity vector
\tilde{W}	Ambipolar velocity vector

List of symbols

Φ	Flux vector
D	Diffusion tensor
FDS	Free diffusion step
TDS	Trapping diffusion step
C	Colman proton concentration
∇C	Concentration gradient vector

Introduction

In previous papers, the orthotropic ambipolar diffusion of (H⁺, e⁻) in γ/ε -MnO₂ in the case of a moderate or a weak reduction degree was studied [1, 2]. Two theories were applied: macroscopic thermodynamics and the analytical theory of heat conduction in an anisotropic medium. The concepts of the instantaneous and continuous point sources were especially exploited. The aim of the present work is to:

1. Continue the study of diffusion [accompanied (or not) with trapping]. The reduction degree is extended up to the value $r = 1$ and the two transport forces (electric/thermodynamic) are taken into account.

H. Kahil
Laboratoire d'Electrochimie Organique et Photochimie Redox,
Université Joseph Fourier, B.P. 68,
38402 Saint Martin d'Hères Cedex, France
Tel.: +33-4-76-407630; e-mail: hkahil@hotmail.com

2. Demonstrate that the internal electric field plays a multiple fundamental role in the dynamics of $\gamma/\varepsilon\text{-MnO}_2$ reduction.
3. Propose for the entire insertion phenomenon an ordinal dynamic modelisation as a function of r .

In this section a wide bibliography is given, followed by a general synthesis on the physico-chemical properties of $\gamma\text{-MnO}_2$.

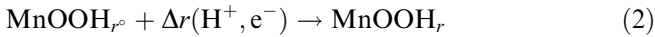
Conceptual basis

Definition

It is well known that $\gamma\text{-MnO}_2$ is an n-semiconductor [3, 4] which is reduced in a homogeneous phase, by incorporation of (H^+, e^-) , according to the equation



or more exactly

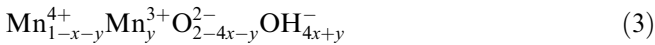


$$r = r^\circ + \Delta r$$

The reactants and products of this reaction constitute an interstitial solid solution “ MnOOH_r ” whose composition and thermodynamic/kinetic characterization has been the subject of controversy. The reduction level r , is defined as the ratio between the numbers of inserted electrons and total manganese ions in the solid phase.

Composition

The most used chemical formula is Rueschi’s model [5]



with $4x\text{OH}^-$ the internal water, $y\text{OH}^-$ “the initially and the inserted” fraction of H^+ and $y\text{Mn}^{3+}$ “the initially and the inserted” fraction of e^- . In the case of a non-reduced electrolytic manganese dioxide international common sample (EMD-ICS) no. 1, we have: $x = 0.065$ and $y^\circ = 0.075$.

Reoxidation

The partly reduced $\gamma\text{-MnO}_2$ can be reoxidised as well if $r < 0.5$ or in a less good manner if $0.5 < r < 0.8$ [6, 7]. Note that according to Kordesch et al. [8, 9], better reoxidation can be obtained when $r < 0.35$.

Position of protons and OH^- ion formation

One can deduce from the results of Fillaux and Tye et al. [10–15] that the inserted protons in $\gamma\text{-MnO}_2$ are still

delocalized up to $r \approx 0.50$ and their behaviour is then approximately similar to a gas of free particles. Nevertheless, the results of these authors diverge in the determination of the r value (level) at which the OH^- ion forms. This level is estimated to be near 0.8 for Tye et al. [10, 15] or close to 0.96 for Fillaux et al. [11–14].

Formation of Mn^{3+} ion

Several papers [16–21] have indicated that some distortion of MnO_6^{9-} by the Jahn-Teller effect occurs in MnO_2 when $r > 0.50$. This property means that the Mn^{3+} ion does not form before this value and the inserted electrons are still in the delocalized state. It is also worth noting that the delocalization concept has been largely discussed by Atlung [22] in terms of an eventual formation of $\text{Mn}_2\text{O}_4\text{H}$ during the reduction reaction of $\gamma\text{-MnO}_2$.

Diffusivity

A first reading of several dynamic results [4, 23, 24] indicates that during an entire reduction reaction of $\gamma\text{-MnO}_2$: $\underline{D}_{\text{H}^+}$ decreases very slowly, $\underline{D}_{\text{e}^-}$ decreases weakly at $0.08 \leq r \leq 0.28$ and very much if $r > 0.28$, and the comparison between $\underline{D}_{\text{e}^-}$ and $\underline{D}_{\text{H}^+}$ gives $\underline{D}_{\text{e}^-}/\underline{D}_{\text{H}^+} \gg 1$.

The correlation between structure and r

It is of great importance to correlate the change in the MnOOH_r properties with different values of r . Therefore, Fitzpatrick and Tye [25] have clearly demonstrated the existence, during a total reduction of $\gamma\text{-MnO}_2$, of four structural steps which are thermodynamically distinguished. Every step is characterized by a value set of the structural parameters and corresponds to an interval of r :

$$\begin{aligned} 0.11 < r < 0.25 \\ 0.25 < r < 0.45 \\ 0.45 < r < 0.80 \\ r > 0.80 \end{aligned}$$

Fillaux et al. [14] have also proposed a dynamic (protonic) classification approximately similar to that of Tye et al.:

$$\begin{aligned} 0.04 < r < 0.30 \\ 0.30 < r < 0.60 \\ 0.60 < r < 0.70 \\ 0.70 < r < 0.80 \\ r > 0.80 \end{aligned}$$

In both cases, a new phase appears for $r > 0.80$.

Thermodynamic potential of $MnOOH_r$

Although it is not the aim of this work, a brief résumé on ε is very useful. First, Tye [26] has demonstrated that the $MnOOH$ formed during a weak reduction of $\gamma\text{-MnO}_2$ dissociates completely (like a strong electrolyte in water) into Mn^{3+} , O^{2-} and OH^- . These three ions constitute with Mn^{4+} an ideal ionic solid solution, whose thermodynamic potential in a non-acidic medium and at constant pH may be expressed (relative to the standard hydrogen electrode immersed in the same electrolyte) as follows:

$$\varepsilon = \varepsilon^{\circ} + 2(RT/F) \ln(1 - r)/r \quad (4)$$

or

$$\Delta\varepsilon = 2(RT/F) \ln(1 - r)/r \quad (5)$$

In a second paper [27], the same authors have demonstrated that the experimental data and the characteristic curve of Eq. (4) are in good agreement over the whole range from $\gamma\text{-MnO}_2$ to $\delta\text{-MnOOH}$. Nevertheless, in the zone $0.38 < r < 0.80$ some divergence between the two graphics appears and gives rise to the difference:

$$\psi(\text{volts}) = \varepsilon(\text{Eq. (4)}) - \varepsilon(\text{experimental}) .$$

Therefore the thermodynamic results of Tye et al. have demonstrated that, during the whole reduction reaction in the homogeneous phase, the strong electrolyte (H^+ , e^-) is continually dissociated into H^+ and e^- . Nevertheless, the existence of factor 2 in Eq. (4) and the difference ψ needs a theoretical interpretation, taking into account most of the $\gamma\text{-MnO}_2$ published data [28]. Notice that we can also find factor 2 in the thermodynamic potential expressions of other protonic systems: $Ni(OH)_2/NiOOH$, Pb/H_xPbO_2 etc. It was interpreted by Barnard et al. [29] as the sign of a ‘‘strong electrolyte’’ dissociation phenomenon. Inversely, factor 1 (instead of 2) indicates the existence of an association (between the inserted particles) phenomenon; this is the (non-electrolytic) case of $\beta\text{-MnO}_2$.

Summary

1. Dissociation of (H^+ , e^-) in $MnOOH_r$. First of all, it is a dynamic phenomenon whose origin can be attributed to the existence of: double tunnels which offer the free space necessary to dissociate, separate and delocalize (H^+ , e^-); and to an important initial concentration in (H^+ , e^-) and the internal electric field (inversely, this latter originates from the same concept, the dissociation; in fact, it is induced by the diffusion, inside the $\gamma\text{-MnO}_2$ network, of two separated particles which have the same concentration but two opposite electrical charges and very different diffusivity mean values) [2]. Notice that in the grain of $\beta\text{-MnO}_2$ which does not have these advantages [double tunnels, vacancies, important ini-

tial concentration in (H^+ , e^-) and a Nernst field] there is no dissociation nor delocalization [2]. From a theoretical point of view [30–34], the dissociation needs the existence of a continuum medium playing the role of a solvent S where the strong electrolyte (H^+ , e^-) can easily dissociate. Thus, one must justify why the $\gamma\text{-MnO}_2$ can be considered as such a medium.

2. Diffusion nature. The last concept does not mean that the (H^+ , e^-) diffusion inside the solid solvent (like the diffusion in a liquid solvent) is isotropic, but surely anisotropic. To study diffusion in such a medium we can apply the analytical theory of heat conduction in an anisotropic solid [1, 35, 36].
3. Trapping or localization of the inserted particles. It takes place inside $MnOOH_r$ when we have $r > 0.50$.
4. Internal electric field. Except for two papers [1, 2], this very important physical phenomenon is completely unexploited in the domain of electrochemical power sources. The study and development of these may be facilitated, as we will see, by the identification of the relation between E_d (when it exists) and the insertion reaction.
5. Rueschi’s formula. It is very important to notice that one has to take into account y° and x every time the mean degree of reduction r is involved. Therefore, all the literature results exploited in this work have been corrected on this basis (see the Appendix).
6. Finally, so far, none of the literature results has confirmed the existence of a direct recombination between H^+ and e^- to give H. Therefore, such a phenomenon is ignored in this work.

Fundamental role of the Nernst field in the behaviour change at $r \approx 0.50$ of $\gamma\text{-MnO}_2$

Exploitation of the diffusivities experimental data

Consider Eqs. (A6)–(A8) in the Appendix describing the variation of \underline{D}_{e^-} and \underline{D}_{H^+} as a function of r , and write them again in the following forms:

For $0.08 \leq r \leq 0.28$

$$(RT/F) \ln(\underline{D}_{e^-}/\underline{D}_{H^+}) \approx 0.2(1 - r) \quad (6)$$

or

$$(RT/F) \ln(\underline{D}_{e^-}/\underline{D}_{H^+})^{1/2} \approx 0.1(1 - r) \quad (7)$$

For $0.28 \leq r \leq 0.50$

$$(RT/F) \ln(\underline{D}_{e^-}/\underline{D}_{H^+}) \approx 0.8(0.5 - r) \quad (8)$$

or

$$(RT/F) \ln(\underline{D}_{e^-}/\underline{D}_{H^+})^{1/2} \approx 0.4(0.5 - r) \quad (9)$$

Equation (9) indicates that at $r \approx 0.50$ we have:

$$\underline{D}_{e^-}/\underline{D}_{H^+} = 1 \quad (10)$$

Applications

In Table 1 (see Appendix) are listed the values of $(RT/F) \ln(\underline{D}_{e^-}/\underline{D}_{H^+})^{1/2}$ and $\Delta\varepsilon$ corresponding to the interval $0.08 \leq r \leq 0.50$. It is seen that in the region $0.08 \leq r \leq 0.28$, we have

$$(RT/F) \ln(\underline{D}_{e^-}/\underline{D}_{H^+})^{1/2} \approx \Delta\varepsilon \quad (11)$$

or

$$(RT/F) \ln(\underline{D}_{e^-}/\underline{D}_{H^+})^{1/2} \approx 2(RT/F) \ln(1-r)/r \quad (12)$$

whereas in the region $0.28 \leq r \leq 0.50$ these equations become

$$(RT/F) \ln(\underline{D}_{e^-}/\underline{D}_{H^+})^{1/2} \approx 2\Delta\varepsilon \quad (13)$$

or

$$(RT/F) \ln(\underline{D}_{e^-}/\underline{D}_{H^+})^{1/2} \approx 4(RT/F) \ln(1-r)/r \quad (14)$$

Equations (6)–(14) and Table 3 (in the Appendix) demonstrate a set of important or fundamental facts:

1. The two mean diffusion coefficients become equal near the mid distance of the total reduction. The most striking in this crossing ($\underline{D}_{e^-} = \underline{D}_{H^+}$) is that it takes place at the point where $C = C_{\max}/2$. This latter explains the equality between the numbers of free and occupied sites, if we suppose that all the inserted particles are trapped. Finally, this result enables us to interpret some of the not-understood characteristics of γ -MnO₂.
2. Except for the median common value (at $r \approx 0.50$), the difference between the \underline{D}_{e^-} and \underline{D}_{H^+} values is important or very important.
3. From the last case of Table 3 ($r > 0.60$) and the published data on γ -MnO₂, one can neglect, as a first approximation, the electronic mean diffusivity value with respect to the protonic one. This fact proves that the Mn³⁺ ion formation is more destructive for the reaction insertion than the proton fixation at the center of the O₆ octahedron [11–14]. In other words, it appears that the pairing phenomenon is more destructive for the electronic network than for the protonic one: the formation of Mn³⁺, accompanied by the Jahn-Teller effect, cuts the continuity of the electronic diffusion network and at $r \approx 0.80$ involves the appearance of a new phase which has been detected by X-ray diffraction (see above).
4. Equations (11) and (13) invite us to understand that the Eq. (5) is the thermodynamic characteristic (or image) of the dynamic quantity $(RT/F) \times \ln(\underline{D}_{e^-}/\underline{D}_{H^+})^{1/2}$.
5. Published value [37, 38], $\underline{D}_{H^+} \approx 10^{-15}$ cm²/s, does not correspond to the good energetic performances of γ -MnO₂. In fact, using it and $\underline{D}_{e^-} \approx 10^{-3}$ cm²/s [4], one can obtain $(RT/F) \ln(\underline{D}_{e^-}/\underline{D}_{H^+})^{1/2} = 0.355$ V, which is very far from the values mentioned in Table 1.

The Nernst field switching over

It is known that \mathbf{E}_d imposes the same mean velocity to the two inserted particles [2]. From the above results one can conclude that the internal electric field accelerates the proton in the interval $0.08 \leq r \leq 0.50$ and slows it down at $0.50 \leq r \leq 1$ (inversely for the electron). Consequently, \mathbf{E}_d possesses two opposed roles during the entire reduction ($0.08 \leq r \leq 1$). This also means that by reversing its orientation, at $r \approx 0.50$, the \mathbf{E}_d intensity must necessarily pass through the zero value. This latter corresponds in fact to the equality between the diffusivities mean values \underline{D}_{e^-} and \underline{D}_{H^+} .

Behaviour change and Mn³⁺ formation at $r \approx 0.50$

This phenomenon is the fundamental consequence of the inversion in the role of the internal electric field with respect to the two inserted particles. Finally, a physical interpretation of trapping will be given below, preceded by an analytical translation of all the above-mentioned results.

Theory

General concepts

MnO₂ continuum solid medium

In Fer's point of view [34], the application of the continuous macroscopic approach to a solid medium, crossed by some matter flux, is possible when the diffusion length has a value of about 0.1 μ m as an order of magnitude. That is the case of the (H⁺, e⁻) diffusion in γ -MnO₂ submitted to the insertion flux. In fact, the mean grain diameter is 30 μ m and the time of use in general is sufficiently high to allow the diffusion length to reach the Fer's order of magnitude.

Anisotropy of diffusion

The γ -MnO₂ is an orthotropic medium [1, 35, 36]. The mutually perpendicular crystallographic axes (\mathbf{a} , \mathbf{b} , \mathbf{c}) of this structure are at the same time the principal ones. They constitute the crystallophysical orthonormed reference frame (O, \mathbf{x} , \mathbf{y} , \mathbf{z}). The diffusion tensor \mathbf{D} can be written as a diagonal matrix $[D_{ii}]$, $i = 1, 2, 3$. It should be noticed that, assuming the grain volume increase during the reaction is still sufficiently weak, the translation of the reference frame can be omitted [27, 35, 39].

Finally, with the aim of making the calculation easier, the "sum and difference" diffusivities tensors are defined as follows:

$$\mathbf{D}_s = \mathbf{D}_{e^-} + \mathbf{D}_{H^+} \quad (15)$$

and

$$D_d = D_{e^-} - D_{H^+} \quad (16)$$

Reduction degree r

From the first section one can write $r = y/(1 - x)$ and, in the “EMD-ICS no. 1” case, $r = y/0.935$. Therefore, r takes values between 0.08 and 1.

Interaction force, trapping/ Mn^{3+} formation

The data mentioned in the first section and the electrolytic theory of the semiconductors (developed by Reiss et al. [31–33]) will now be applied. The coulombic interaction force, working in the “ H^+ , e^- , S” system, may be:

1. Negligible (up to $r \approx 0.38$); the solid solution is then ideal.
2. Weak or of “Debye and Hückel” kind. It participates in the transport phenomenon but its low intensity does not permit pair formation. This force, which will be designated by F' , is an increasing function of the concentration C (see below). Finally, it is evident that the present case is extended in the region $0.38 < r < 1$ and implies the non-ideality of the solid solution ($f_{H^+} < 1$ and $f_{e^-} < 1$).
3. Important, which gives rise to the pairing phenomenon. This interaction kind does not exclude the former (2) but it is so intense that one can consider it as the only interaction governing the pairs distribution. Nevertheless, the weak interaction (2) must be calculated for the unpaired ions.

Finally, in the next sections, pairing and trapping will explain the same phenomenon: the localization of the diffusing particles.

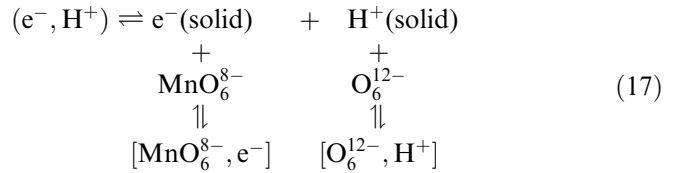
Principal dynamic steps

Based on the above analysis, one can consider that the two inserted particles H^+ and e^- have, simultaneously, the same physical behaviour which is imposed by the electric neutrality and the Nernst field: diffusion without trapping or diffusion with trapping. Therefore, one can propose the two following main steps:

1. Free diffusion step (FDS), $0.08 < r < 0.50$. The inserted protons and electrons are approximately in a delocalized state. Then, they have a similar behaviour to gas particles inside which there can exist (or not) a “Debye and Hückel” interaction. Notice here that Eq. (2) represents well the reaction mechanism of the FDS.
2. Non-free (or trapping) diffusion step (TDS), $0.50 < r < 1$. This phenomenon takes place at $r \approx 0.50$. The inserted protons and electrons may be trapped in O_6 and MnO_6 octahedrons and the

$[O_6^{12-}, H^+]$ or $[MnO_6^{8-}, e^-]$ pairs can be formed (this latter will be considered approximately in the next paragraphs, as a Mn^{3+} ion). In fact, the crystalline structure appears as acting with its two half O_6 octahedrons: one serves to trap the electrons with its Mn^{4+} nucleus, and other fixes the protons in its unoccupied center [11–14].

Because it does not take into account the pairing phenomenon, Eq. (2) must be replaced by:



The first line of Eq. (17) indicates that the dissociation of the strong electrolyte (e^- , H^+) always takes place (inside the homogeneous phase), at least up to the total reduction of its manganese (+IV) ions. The second line designates well the chemical identity of the traps and considers that they have approximately (see Rueschi’s formula) the same concentration C' . The third line identifies the reaction products. The matter conservation law imposes the same concentration “ P ” to the formed pairs. These latter must be considered as they are juxtaposed or at least neighbours.

Principal dynamic quantities of insertion

Various physical quantities which govern the insertion in γ - MnO_2 will be defined and briefly studied throughout this section.

Free diffusion step

Ionic force. Like the case of the diluted aqueous solutions, one can consider that the activity coefficients of protons or electrons only depend on the ionic force I of the solid solution “S, H^+ , e^- ” [40]:

$$I = (1/2) \sum_i C_i z_i^2 \quad (18)$$

where z_i is the electrical charge number of the ion i . Because of the fact that the concentrations and charge numbers of protons and electrons are equal, Eq. (18) becomes:

$$I = C_{H^+} = C_{e^-} = C \quad (19)$$

From Eq. (19) one can deduce that the activity coefficients f_{H^+} and f_{e^-} are only concentration C dependent.

Thermodynamic transport force. During the insertion reaction there is a progressive increase in the concentration C . As we have mentioned (see above), the coulombic interactions exchanged between the inserted

particles, or between them and the solvent, provokes the progressive removal of the solid solution from the ideal state. Consequently, the value of f (or $\ln f$) decreases progressively and yields a force \mathbf{F}' which opposes the augmentation of C and thus the flux of the inserted particles. In fact, \mathbf{F}' is the thermodynamic transport force defined [1, 39] by

$$\mathbf{F}' = -kT\nabla(\ln f) \quad (20)$$

or

$$\mathbf{F}' = -kT(\partial \ln f / \partial C) \nabla C \quad (21)$$

The coefficient f (or $\ln f$) increases inside the continuum medium in the opposed orientation of ∇C , i.e. from the grain surface to its bulk. The force \mathbf{F}' is then parallel to the concentration gradient vector and equally oriented from the interior towards the surface of the grain.

General expression of the flux. Taking into account the influence of the concentration gradient and the two transport forces, one can define the flux vectors as follows [1, 39, 41–44]:

$$\Phi_{\text{H}^+} = -[1 - (eC/kT)\mathbf{E}_d/\nabla C + C\partial \ln f_{\text{H}^+}/\partial C]\mathbf{D}_{\text{H}^+}\nabla C \quad (22)$$

and

$$\Phi_{\text{e}^-} = -[1 + (eC/kT)\mathbf{E}_d/\nabla C + C\partial \ln f_{\text{e}^-}/\partial C]\mathbf{D}_{\text{e}^-}\nabla C \quad (23)$$

(Note that the ratio between two vectors ($\mathbf{E}_d/\nabla C$) it is not well defined from a mathematical point of view, but it must be adopted here for practical reasons.)

General expression of the orthotropic ambipolar diffusion tensor $\tilde{\mathbf{D}}$. Now let, $\tilde{\mathbf{D}}_{\text{H}^+}$ and $\tilde{\mathbf{D}}_{\text{e}^-}$ be defined by the following:

$$\Phi_{\text{H}^+} = -\tilde{\mathbf{D}}_{\text{H}^+}\nabla C \quad (24)$$

and

$$\Phi_{\text{e}^-} = -\tilde{\mathbf{D}}_{\text{e}^-}\nabla C \quad (25)$$

Using Eqs. (22) and (23) one can obtain

$$\tilde{\mathbf{D}}_{\text{H}^+} = [1 - (eC/kT)\mathbf{E}_d/\nabla C + C\partial \ln f_{\text{H}^+}/\partial C]\mathbf{D}_{\text{H}^+} \quad (26)$$

and

$$\tilde{\mathbf{D}}_{\text{e}^-} = [1 + (eC/kT)\mathbf{E}_d/\nabla C + C\partial \ln f_{\text{e}^-}/\partial C]\mathbf{D}_{\text{e}^-} \quad (27)$$

It should be remarked here that in the expression of every ambipolar tensor appear all the parameters and physical quantities of the insertion dynamics.

Ambipolar velocity. Write now Eqs. (24) and (25) as follows:

$$\Phi_{\text{H}^+} = C(-\tilde{\mathbf{D}}_{\text{H}^+}\nabla C/C)$$

and

$$\Phi_{\text{e}^-} = C(-\tilde{\mathbf{D}}_{\text{e}^-}\nabla C/C)$$

The terms enclosed in parentheses have the dimensions of a velocity vector ($\tilde{\mathbf{W}}$). Then:

$$\tilde{\mathbf{W}}_{\text{H}^+} = -\tilde{\mathbf{D}}_{\text{H}^+}\nabla C/C \quad (28)$$

and

$$\tilde{\mathbf{W}}_{\text{e}^-} = -\tilde{\mathbf{D}}_{\text{e}^-}\nabla C/C \quad (29)$$

The last relations represent the ambipolar velocity of the inserted proton or electron.

Self velocity. We now introduce two new physical quantities, specific to the proton and electron, with their vectorial difference or sum:

$$\mathbf{V}_{\text{H}^+} = -(1/C + \partial \ln f_{\text{H}^+}/\partial C)\mathbf{D}_{\text{H}^+}\nabla C \quad (30)$$

$$\mathbf{V}_{\text{e}^-} = -(1/C + \partial \ln f_{\text{e}^-}/\partial C)\mathbf{D}_{\text{e}^-}\nabla C \quad (31)$$

$$\mathbf{V}_d = \mathbf{V}_{\text{e}^-} - \mathbf{V}_{\text{H}^+} = -[(1/C)\mathbf{D}_d + (\partial \ln f_{\text{e}^-}/\partial C)\mathbf{D}_{\text{e}^-} - (\partial \ln f_{\text{H}^+}/\partial C)\mathbf{D}_{\text{H}^+}]\nabla C \quad (32)$$

and

$$\mathbf{V}_s = \mathbf{V}_{\text{e}^-} + \mathbf{V}_{\text{H}^+} = -[(1/C)\mathbf{D}_s + (\partial \ln f_{\text{e}^-}/\partial C)\mathbf{D}_{\text{e}^-} + (\partial \ln f_{\text{H}^+}/\partial C)\mathbf{D}_{\text{H}^+}]\nabla C \quad (33)$$

In fact, we have here a regrouping of the diffusional and thermodynamic components for every inserted particle. \mathbf{V}_{e^-} and \mathbf{V}_{H^+} have the dimensions of a velocity vector which can be called the self or thermodiffusional velocity. It explains the swiftness of a particle, diffusing alone under the influence of the two following potential factors: bulk/capacitive, $(1/C)\mathbf{D}\nabla C$, and interactive, $(\partial \ln f/\partial C)\mathbf{D}\nabla C$.

It is important (for the next paragraphs) to remark that: \mathbf{V}_d seems to be the relative velocity of the electron with respect to the proton, and that $\mathbf{V}_s/2$ may be considered as the vectorial mean of the self velocities (\mathbf{V}_{e^-} and \mathbf{V}_{H^+}) or the mean self velocity of the (e^- , H^+) couple into the solid phase.

Finally, as the next equations will demonstrate, the principal interest of the above four regroupings [Eqs. (30)–(33)] is the fact that they can appear explicitly as the “electronic or protonic” components in the expressions of \mathbf{E}_d , Φ and $\tilde{\mathbf{W}}$. This procedure is attractive from the physical point of view and makes the mathematics more concise.

General analytical expression of the internal electric field. The electric neutrality of the orthotropic medium imposes:

$$\Phi_{\text{e}^-} = \Phi_{\text{H}^+} = \Phi \quad (34)$$

From Eqs. (24)–(34) one can obtain the following ambipolar equalities:

$$\tilde{\mathbf{D}}_{\text{H}^+} = \tilde{\mathbf{D}}_{\text{e}^-} = \tilde{\mathbf{D}} \quad (35)$$

$$\tilde{W}_{H^+} = \tilde{W}_{e^-} = \tilde{W} \quad (36)$$

with

$$\tilde{W} = -\tilde{D}\nabla C/C = C^{-1}\Phi \quad (37)$$

and the general analytical expression of the Nernst field

$$\begin{aligned} E_d &= -(kT/e)\{D_d/C + [(\partial \ln f_{e^-}/\partial C)D_{e^-} \\ &\quad - (\partial \ln f_{H^+}/\partial C)D_{H^+}]\}D_s^{-1}\nabla C \\ &= (kT/e)D_s^{-1}V_d \end{aligned} \quad (38)$$

The magnitude of the ambipolar vector \tilde{W} is inversely proportional to C but is proportional to the ambipolar diffusion tensor and to ∇C , and has an orientation which is, in a way, opposed to ∇C .

Finally, because it correlates the principal dynamic quantities of the insertion, Eq. (37) is then of great importance.

Equation (38) proves well that the Nernst field is proportional to the V_d vector but inversely proportional to the diffusion sum tensor. Consequently, the existence of E_d is due to the more general difference between the protonic and electronic self velocities. On the other hand, from Eq. (38), which contains the ∇C factor, one can deduce that \tilde{D} , as it is defined by Eq. (26) or (27), is independent of ∇C .

To sum up, E_d opposes the dynamic non-homogeneity inside the γ -MnO₂ grain, realises the coupling between the electronic and protonic flux and obliges the inserted particles to diffuse with the common diffusion tensor (\tilde{D}) and velocity (\tilde{W}).

Boundary conditions. Evidently the two self velocities must have an orientation which is, in a way, opposed to that of ∇C , which means that Eqs. (30) and (31) must verify the two following conditions:

$$1/C + \partial \ln f_{e^-}/\partial C > 0$$

and

$$1/C + \partial \ln f_{H^+}/\partial C > 0$$

$$\partial \ln(f_{H^+}) > -\partial C/C \text{ (with } \partial C > 0 \text{)}$$

$$\ln(f_{H^+}) > \ln bC^{-1} \text{ (} b \text{ is constant)}$$

$$bC^{-1} < f_{H^+} < 1$$

but at $t = 0$ we have (see earlier), $f_{H^+} = 1$. Then $b < C^\circ$ where C° is the initial concentration. By putting (in order to simplify) $b \approx C^\circ$, one can obtain the following boundary condition:

$$C^\circ/C < f_{H^+} < 1 \quad (39)$$

Similarly

$$C^\circ/C < f_{e^-} < 1 \quad (40)$$

Finally, at $r = 0.50$, where $C \approx 6.3C^\circ$. (See A₁), one can write Eqs. (39) and (40) as follows:

$$0.16 < f_{H^+} < 1$$

and

$$0.16 < f_{e^-} < 1$$

Non-free diffusion case

The same dynamic quantities defined above (in FDS) will be used also in this step, TDS. It is evident that taking trapping into account will introduce some modifications in the analytical expressions.

Preliminary equations. Admitting that the three chemical quantities e^- , MnO_6^{8-} and $[MnO_6^{8-}, e^-]$ are in dynamic equilibrium [33], it follows from Eq. (17) that:

$$\Omega = P/(C - P)(C' - P) \quad (41)$$

and thus

$$\begin{aligned} (C - P) &= (1/2)(C - C' - 1/\Omega) \\ &\quad + [(1/4)(C - C' - 1/\Omega)^2 + C/\Omega]^{1/2} \end{aligned} \quad (42)$$

Therefore one can easily demonstrate that

$$\begin{aligned} \nabla(C - P) &= (1/2) \\ &\quad \times \left[1 + \frac{(1/2)(C - C' + 1/\Omega)}{[(1/4)(C - C' - 1/\Omega)^2 + C/\Omega]^{1/2}} \right] \\ &\quad \times \nabla C \end{aligned} \quad (43)$$

and then

$$\nabla(C - P) = h\nabla C \quad (44)$$

with the coefficient

$$h = (1/2) \left[1 + \frac{(1/2)(C - C' + 1/\Omega)}{[(1/4)(C - C' - 1/\Omega)^2 + C/\Omega]^{1/2}} \right] \quad (45)$$

At the same time, Eqs. (41)–(45) also represent the dynamic equilibrium between the other three chemical quantities H^+ , O_6^{12-} and $[O_6^{12-}, H^+]$.

From Eqs. (43)–(45) it can be remarked that:

1. $0 < h \leq 1$, the coefficient h tends to unity when P approaches zero (r approaches 0.50).
2. $|\nabla(C - P)| < |\nabla(C)|$; therefore the number of mobile particles will always be smaller than the numbers of inserted particles. Consequently, the matter (H) quantity transferred by the concentration gradient on TDS is lower than the one we have on FDS.

Dynamic quantities expressions. Replacing in Eqs. (22)–(27) the quantities C , ∂C and ∇C respectively by $(C - P)$, $h\partial C$ and $h\nabla C$, they become:

$$\begin{aligned} \Phi_{e^-} &= -\tilde{D}_{e^-}\nabla(C - P) = -\{h + e(C - P)E_d/kT\nabla C \\ &\quad + (C - P)\partial \ln f_{e^-}/\partial C\}D_{e^-}\nabla C \end{aligned} \quad (46)$$

$$\begin{aligned} \Phi_{H^+} &= -\tilde{D}_{H^+}\nabla(C - P) = -\{h - e(C - P)E_d/kT\nabla C \\ &\quad + (C - P)\partial \ln f_{H^+}/\partial C\}D_{H^+}\nabla C \end{aligned} \quad (47)$$

$$\begin{aligned} \tilde{\mathbf{D}}_{e^-} = & \{1 + e(C - P)\mathbf{E}_d/kTh\nabla C \\ & + [(C - P)/h]\partial \ln f_{e^-}/\partial C\}\mathbf{D}_{e^-} \end{aligned} \quad (48)$$

and

$$\begin{aligned} \tilde{\mathbf{D}}_{H^+} = & \{1 - e(C - P)\mathbf{E}_d/kTh\nabla C \\ & + [(C - P)/h]\partial \ln f_{H^+}/\partial C\}\mathbf{D}_{H^+} \end{aligned} \quad (49)$$

where $\tilde{\mathbf{D}}$ is the ambipolar TDS tensor (diffusion with trapping), and \mathbf{D} corresponds here to the total concentration (without trapping).

The ambipolar velocities can be obtained from previous relations [Eqs. (46)–(49)], as follows:

$$\begin{aligned} \tilde{\mathbf{W}}_{H^+} = & [1/(C - P)]\Phi_{H^+} \\ \text{or} \\ \tilde{\mathbf{W}}_{H^+} = & -h\tilde{\mathbf{D}}_{H^+}\nabla C/(C - P) \end{aligned} \quad (50)$$

and

$$\begin{aligned} \tilde{\mathbf{W}}_{e^-} = & [1/(C - P)]\Phi_{e^-} \\ \text{or} \\ \tilde{\mathbf{W}}_{e^-} = & -h[1/(C - P)]\tilde{\mathbf{D}}_{e^-}\nabla C \end{aligned} \quad (51)$$

Finally, with the electric neutrality condition, one can obtain the expression of the Nernst field:

$$\begin{aligned} \mathbf{E}_d = & -[kT/e]\{h\mathbf{D}_d/(C - P) + \mathbf{D}_{e^-}(\partial \ln f_{e^-}/\partial C) \\ & - \mathbf{D}_{H^+}(\partial \ln f_{H^+}/\partial C)\}\mathbf{D}_s^{-1}\nabla C = [kT/e]\mathbf{D}_s^{-1}\mathbf{V}_d \end{aligned} \quad (52)$$

with

$$\mathbf{V}_{e^-} = -[h/(C - P) + \partial \ln f_{e^-}/\partial C]\mathbf{D}_{e^-}\nabla C \quad (53)$$

$$\mathbf{V}_{H^+} = -[h/(C - P) + \partial \ln f_{H^+}/\partial C]\mathbf{D}_{H^+}\nabla C \quad (54)$$

and

$$\begin{aligned} \mathbf{V}_d = & -[h(C - P)^{-1}\mathbf{D}_d + (\partial \ln f_{e^-}/\partial C)\mathbf{D}_{e^-} \\ & - (\partial \ln f_{H^+}/\partial C)\mathbf{D}_{H^+}]\nabla C \end{aligned} \quad (55)$$

$$\begin{aligned} \mathbf{V}_s = & -[h(C - P)^{-1}\mathbf{D}_s + (\partial \ln f_{e^-}/\partial C)\mathbf{D}_{e^-} \\ & + (\partial \ln f_{H^+}/\partial C)\mathbf{D}_{H^+}]\nabla C \end{aligned} \quad (56)$$

It is important to notice here that the Nernst electric field has the same expression in both the steps FDS and TDS.

The longitudinal and transversal components roles of the vectorial quantities

The concentration gradient ∇C , in a given point \mathbf{M} is always oriented towards the outward of the γ - MnO_2 grain [1]. With the exception of the principal axes directions, the five vectors “ $-\mathbf{D}\nabla C$ ”, \mathbf{E}_d , Φ , \mathbf{V} and $\tilde{\mathbf{W}}$ do not lie in the direction of ∇C . Thus, every vectorial quantity \mathbf{G} , implicated in the insertion reaction, has generally along ∇C two components:

1. Longitudinal \mathbf{G}_l , which can contribute positively (or not) to the matter transfer, depending if it is lying (or not) in the direction of “ $-\nabla C$ ” [The vector “ $-\nabla C$ ”

indicates, in fact, the positive orientation of the (effective) matter transfer during the insertion reaction; it represents the principal potential factor in the diffusion phenomenon].

2. Transversal \mathbf{G}_t , whose role is to make more homogeneous the distribution (around the “ $-\nabla C$ ” direction) of the matter transferred by the longitudinal component \mathbf{G}_l .

Physical interpretation of the Nernst field role in the pairing phenomenon

The essential new point to be made, from the previous results, is that the \mathbf{E}_d orientation forbids the pair formation on FDS but allows it on TDS (after the reversing of its orientation at $r \approx 0.50$, see above). It can be interpreted as follows:

1. FDS. While the longitudinal component \mathbf{E}_{ld} slows down the electron movement and accelerates the protonic one, the transversal component \mathbf{E}_{td} , repulses the electrons far from the MnO_6^{8-} octahedrons, especially when C is not important.
2. TDS. Along this step, we have the inverse phenomenon. In fact, H^+ is slowed down while e^- is accelerated by \mathbf{E}_{ld} . The transversal component \mathbf{E}_{td} attracts the electrons towards the MnO_6^{8-} octahedrons and offers to them the two energies α_1 and α_2 necessary to: jump the potential barrier existing at the octahedron surface, and penetrate inside it, towards the Mn^{4+} ion; reduce the Mn^{4+} ion. The absorption of an electron by the latter implies the famous distortion of MnO_6 (Jahn-Teller effect). The total energy α involved in the formation of Mn^{3+} is then:

$$\alpha = \alpha_1 + \alpha_2$$

The global energy necessary to the formation of N Mn^{3+} pairs is then

$$E \approx \sum_1^N \alpha_i \quad (57)$$

The proton fixation inside the octahedron O_6 [11–14] must be considered as the result of three factors: the repulsion exercised by \mathbf{E}_{ld} which absorbs some part of its energy, the negative charge of O_6 and the existence of a neighbour trapped electron. This means that the formation of a $[\text{MnO}_6^{8-}, e^-]$ pair implies the $[\text{O}_6^{12-}, \text{H}^+]$ neighbour one. This result is the same that Tye [10] had interpreted as the “some association” effect between the particles H^+ and e^- which appears when $r > 0.50$.

Ordinal study of the insertion dynamic regimes

Ordinal variable

The aim of this section is to study at $0.08 \leq r \leq 1$ the variations of the dynamic quantities defined in the pre-

vious section. As mentioned in the latter, the electrolytic theory of semiconductors [31–33] indicates that the role played by the $\partial \ln f / \partial C$ factor (in the variations of the dynamic quantities of the insertion) is of secondary importance compared with the role played by the tensors \mathbf{D}_{H^+} , \mathbf{D}_{e^-} and \mathbf{D}_{d} . Therefore, D_{iid} will be considered, in the following paragraphs, as the principal dynamic variable. D_{iid} represents in fact the relative diffusivity of the electron with respect to the proton, but its variations law, as a function of the independent variable r or C , is unknown. Thus, D_{iid} will be treated as an ordinal variable [45]. It follows that (see above) during the total reduction of $\gamma\text{-MnO}_2$ a set of five successive ordinal modalities

$$D_{\text{iid}} \gg 0, D_{\text{iid}} > 0, D_{\text{iid}} \approx 0, D_{\text{iid}} < 0, D_{\text{iid}} \ll 0 \quad (58)$$

is then imposed. Corresponding to “five intervals of r values”, the set (58) constitutes, in fact, the ordinal scale on which the values of the variable D_{iid} can be measured. As a first approximation, the three ordinal variables $D_{\text{iid}}(i = 1, 2, 3)$ are supposed to take the same ordinal value at the same time, and then they can be measured on the same ordinal scale. Consequently, the dimensions of our problem are reduced from three to one. In other words, the set (58) will be used throughout this part as the measurement scale for only one variable D_{iid} . Certainly this great simplification is due to the use of an ordinal approach.

The determination of the five intervals of r values is obtained from the combination of the approximate results of the Appendix and dynamic/structural thermodynamic classifications (see above). The taking into account of these latter may be justified by considering that the thermodynamic steps are the images (or characteristics) of the dynamic ones (see above). Finally, the modality $D_{\text{iid}} \approx 0$ is defined on an interval Δr centered at $r_{\text{d}} = 0.50$. The value of Δr must be weak, because D_{iid} varies very quickly in this region.

Definition of the dynamic regimes

Now let us define the five dynamic regimes on the basis of all the above and the Appendix results:

FDS

I. $D_{\text{iid}} \gg 0$, $f_{\text{H}^+} = 1$, $f_{\text{e}^-} = 1$ and $0.08 \leq r \leq 0.28$

II. $D_{\text{iid}} > 0$, $0.28 \leq r \leq r_{\text{d}} - \Delta r/2$, with $f_{\text{H}^+} = 1$,
 $f_{\text{e}^-} = 1$ at $0.28 \leq r \leq 0.38$, and $f_{\text{H}^+} < 1, f_{\text{e}^-} < 1$ at
 $0.38 \leq r \leq r_{\text{d}} - \Delta r/2$

III. $D_{\text{iid}} \approx 0$, $f_{\text{H}^+} < 1, f_{\text{e}^-} < 1$ and $r_{\text{d}} - \Delta r/2 \leq r \leq r_{\text{d}} + \Delta r/2$

TDS

IV. $D_{\text{iid}} < 0$, $f_{\text{H}^+} < 1, f_{\text{e}^-} < 1$ and $0.50 < r < 0.60$

V. $D_{\text{iid}} \ll 0$, $f_{\text{H}^+} < 1, f_{\text{e}^-} < 1$ and $0.60 < r < 1$ (59)

Evidently there is some error in every determined value, but this fact does not diminish the theoretical

interest of this ordinal study. It is very important to notice that during the total reduction reaction, every volume element of the $\gamma\text{-MnO}_2$ grain will pass inevitably by the five dynamic regimes. Nevertheless, it is very possible to have several regions (or elementary volumes) in the grain which are submitted to different regimes. Certainly this fact depends on the imposed concentration gradient and the mean distance of every region to the different active sites s_i [1]. In addition, the duration of every regime also depends on these same factors. In the case of a very weak current intensity, the particles H^+ and e^- penetrate, across the reactive sub-surface s_i , with a very small number and without interaction. Therefore, the lifetime of every regime is then important or maximal. Inversely, if the current or gradient intensity is important, the interfacial regions adjacent to s_i become very concentrated and traverse quickly the five regimes: the flux tends quickly to zero and the yield is poor. Clearly, between these two extreme situations there are several intermediate ones.

Regime I

During this regime the solid solution is still near the ideal state, then the logarithmic terms are negligible and the general equations (see above) become:

$$\mathbf{E}_{\text{d}} \approx -(kT/e)\nabla C/C \quad (60)$$

$$\Phi_{\text{H}^+} = \Phi_{\text{e}^-} = -2\mathbf{D}_{\text{H}^+}\nabla C \quad (61)$$

$$\tilde{\mathbf{W}} = -2\mathbf{D}_{\text{H}^+}\nabla C/C \quad (62)$$

with

$$\tilde{\mathbf{D}} = 2\mathbf{D}_{\text{H}^+} \quad (63)$$

Using the expressions of the self velocities \mathbf{V}_{e^-} and \mathbf{V}_{H^+} , it follows that:

$$\mathbf{V}_{\text{e}^-} = -\mathbf{D}_{\text{e}^-}(\nabla C/C) \quad (64)$$

$$\mathbf{V}_{\text{H}^+} = -\mathbf{D}_{\text{H}^+}(\nabla C/C) \quad (65)$$

$$\mathbf{V}_{\text{d}} \sim \mathbf{V}_{\text{e}^-} \quad (66)$$

$$\mathbf{E}_{\text{d}} \approx (kT/e)\mathbf{D}_{\text{e}^-}^{-1}\mathbf{V}_{\text{e}^-} \quad (67)$$

or

$$\mathbf{E}_{\text{d}} \approx (kT/e)\mathbf{D}_{\text{H}^+}^{-1}\mathbf{V}_{\text{H}^+} \quad (68)$$

$$\Phi_{\text{e}^-} = \Phi_{\text{H}^+} = 2C\mathbf{V}_{\text{H}^+} \quad (69)$$

$$\tilde{\mathbf{W}} = 2\mathbf{V}_{\text{H}^+} \quad (70)$$

Corresponding to a negligible thermodynamic force, this regime has been studied in previous papers [1, 2]. The ambipolar diffusivity or velocity ($\tilde{\mathbf{D}}$ or $\tilde{\mathbf{W}}$) is twice the protonic one (\mathbf{D}_{H^+} or \mathbf{V}_{H^+}). This fact demonstrates that, during this regime, the protonic velocity is the governing factor in the (H^+ , e^-) diffusion into $\gamma\text{-MnO}_2$. The internal electric field is created by a difference of several orders of magnitude between the two diffusivities (D_{iH^+} and D_{ie^-}) values and by an important initial concen-

tration of (H^+ , e^-). This regime deserves well to have the appellation ‘‘ideal’’ because it does not only correspond to an ideal solid solution but also to the optimum values of E_d , Φ_{H^+} , Φ_{e^-} (for a given ∇C).

Applications

As matter of great interest, Eqs. (65) and (70) can be used to estimate the ambipolar velocity at the beginning of the insertion [24]:

$$\underline{D}_{H^+} \approx 6 \times 10^{-10} \text{ cm}^2/\text{s}$$

$$|\nabla C| \approx C^\circ/\rho$$

$$\rho \sim 15 \times 10^{-4} \text{ cm}$$

$$C \approx C^\circ$$

$$|\tilde{W}| \approx -2\underline{D}_{H^+}|\nabla C|/C \sim 2\underline{D}_{H^+}/\rho$$

thus

$$|\tilde{W}| \approx 8 \times 10^{-7} \text{ cm/s}$$

Then the necessary time, in the ideal regime, for a given inserted particle to traverse one radius distance is:

$$t \approx \rho/|\tilde{W}| \approx 1875 \text{ s or } 31.3 \text{ min.}$$

The latter order of magnitude appears to be reasonable and agrees well with the published data [46–51]. It is, in fact, the minimal necessary time which permits the flux to reach the grain center and implies the transition from the semi-infinite to the finite diffusion case [1].

It is interesting also to repeat the same calculation with the value of $10^{-15} \text{ cm}^2/\text{s}$, sometimes adopted in the literature [37, 38]. The obtained values are then:

$$|\tilde{W}| \approx 10^{-12} \text{ cm/s}$$

and

$$t \approx 15 \times 10^8 \text{ s or } 2.5 \times 10^7 \text{ min}$$

This infinite time proves that the order of magnitude, $10^{-15} \text{ cm}^2/\text{s}$, does not agree with the proton dynamics in the good electrode material $\gamma\text{-MnO}_2$.

Regime II

Consider a grain region where we have $D_{iiH^+} < D_{iie^-}$. Notice here that E_d is still represented by its general formula of Eq. (38).

Ionic solid solution near the ideal case, $f \approx 1$

The dynamic relations (see above) become respectively:

$$V_d = -D_d \nabla C / C \quad (71)$$

$$\Phi_{H^+} = C[1 + D_d D_s^{-1}] V_{H^+} \quad (72)$$

$$\Phi_{e^-} = C[1 - D_d D_s^{-1}] V_{e^-} \quad (73)$$

The equality between the two flux gives

$$\Phi_{H^+} = \Phi_{e^-} = C[V_s - D_d D_s^{-1} V_d] / 2 \quad (74)$$

and

$$\tilde{W} = [V_s - D_d D_s^{-1} V_d] / 2 \quad (75)$$

The comparison between Eqs. (71)–(75) and (65)–(70) indicates an important decrease in the intensities of the electric field and the flux.

Non-ideal ionic solid solution

By taking Eqs.(22), (23) and (30), (31) into account one can obtain:

$$\Phi_{e^-} = \Phi_{H^+} = C D_s^{-1} [D_{H^+} V_{e^-} + D_{e^-} V_{H^+}] \quad (76)$$

$$\tilde{W} = D_s^{-1} [D_{H^+} V_{e^-} + D_{e^-} V_{H^+}] \quad (77)$$

Equations (76) and (77) demonstrate clearly the dynamic coupling between the movements of H^+ and e^- which is due to the action of the diffusion operators D_{H^+} and D_{e^-} on the vectors V_{e^-} and V_{H^+} .

Regime III

From the data of this regime, one can write the following relations:

$$D_{H^+} \approx D_{e^-} \approx D'$$

$$V_{e^-} = -(1/C + \partial \ln f_{e^-} / \partial C) D' \nabla C \quad (78)$$

$$V_{H^+} = -(1/C + \partial \ln f_{H^+} / \partial C) D' \nabla C \quad (79)$$

$$V_d = -[(\partial \ln(f_{e^-} / f_{H^+}) / \partial C)] D' \nabla C \quad (80)$$

$$V_s = -(2/C + \partial \ln(f_{e^-} f_{H^+}) / \partial C) D' \nabla C \quad (81)$$

$$E_d \approx (kT/2e) D'^{-1} V_d \quad (82)$$

or

$$E_d \approx -(kT/2e)[(\partial \ln(f_{e^-} / f_{H^+}) / \partial C)] \nabla C \quad (83)$$

$$\Phi_{e^-} = \Phi_{H^+} = (1/2) C V_s \quad (84)$$

$$\tilde{W} = (1/2) V_s \quad (85)$$

The ambipolar velocity and the flux are respectively the vectorial mean of the two self velocities or flux (electronic and protonic). With the possible orientations of V_d , one can have the three following cases (see above).

V_d is a ‘‘positive’’ vector

Although it becomes very weak, the electric field always continues to accelerate the proton. Equation (80) must obey the following condition:

$$\partial \ln(f_{e^-} / f_{H^+}) / \partial C > 0$$

$$\partial \ln f_{e^-} / \partial C > \partial \ln f_{H^+} / \partial C$$

$$f'_{e^-} / f'_{H^+} > f_{e^-} / f_{H^+} > 0 \quad (86)$$

(where $f' = \partial f / \partial C$)

f'_{e^-} and f'_{H^+} have the same sign, which means that the variations of f_{e^-} and f_{H^+} are affected in the same orientation (strictly decreasing most probably).

$$V_d = 0 \text{ or } V_{e^-} = V_{H^+}$$

This relation implies that:

$$f_{H^+} = f_{e^-} \quad (87)$$

$$E_d = 0 \quad (88)$$

$$\Phi_{H^+} = \Phi_{e^-} = -C[1/C + f'_{H^+}/f_{H^+}]D'\nabla C \quad (89)$$

$$\tilde{W} = V_{e^-} = V_{H^+} \quad (90)$$

The electric field and the flux coupling are null. The activity coefficients are equal, and it is the same for the self and ambipolar velocities. Equation (89) must obey the condition

$$1/C + f'_{H^+}/f_{H^+} > 0$$

which is equivalent to Eq. (39) or (40).

V_d is a "negative" vector

After its taking a null value, the Nernst field changes its role and increases in intensity. It accelerates the electrons and slows down the protons. Finally, in the present case we must have

$$\partial \ln(f_{e^-}/f_{H^+})/\partial C < 0$$

$$\partial \ln f_{e^-}/\partial C < \partial \ln f_{H^+}/\partial C$$

$$f_{e^-} < f_{H^+}$$

This latter relation indicates that the electron polarisation is more important than the proton one.

Résumé of the evolution on FDS

The injection inside a continuum medium of two ambipolar particles having initially the same concentration, but an important difference between their self velocities, induces a Nernst field which:

1. Couples their movements.
2. Imposes a continuous exchange of the kinetic energy between the two particles up to $r \approx 0.50$, where the self velocities become equal. At this moment, E_d becomes null and the two particles share equally their characteristics

$$(D_{H^+} = D_{e^-}, f_{H^+} = f_{e^-}, \Phi_{H^+} = \Phi_{e^-}, \text{ and } V_{e^-} = V_{H^+} = \tilde{W})$$

Regime IV

The mathematical equations describing the situation in this regime have been developed above. The two self

velocities are again different. The electrons' movement is now less rapid than the protons' one. Consequently, the internal electric field reappears (in an opposed orientation) and exercises its regulator velocity role.

Boundary conditions. Proceeding as in the section entitled "Free diffusion step" (See above), put:

$$b''(C - P)^{-1} < f_{H^+} < 1$$

then, at $t = 0$, i.e. at $r \approx 0.50$, we have $f_{H^+} = f_{e^-} = f'$, $P = 0$ and $C \approx 6.3C^\circ$. Thus

$$6.3C^\circ f'/(C - P) < f_{H^+} < 1 \quad (91)$$

and similarly

$$6.3C^\circ f'/(C - P) < f_{e^-} < 1 \quad (92)$$

Finally, if $f' = 1/6.3$, Eqs. (91) and (92) give

$$C^\circ/(C - P) < f_{H^+} < 1$$

and

$$C^\circ/(C - P) < f_{e^-} < 1$$

Regime V

The equations in the section entitled "Non-free diffusion case" (see above) become:

$$V_d = -[h(C - P)^{-1} + (\partial \ln f_{H^+}/\partial C)]D_{H^+}\nabla C \quad (93)$$

$$V_s = -[h(C - P)^{-1} + (\partial \ln f_{H^+}/\partial C)]D_{H^+}\nabla C \quad (94)$$

Thus

$$E_d \approx [kT/e]D_{H^+}^{-1}V_d \quad (95)$$

As is mentioned above, during this regime a new phase appears progressively. It is not the aim of this work to study this phenomenon.

Summary on the insertion dynamics in $\gamma\text{-MnO}_2$

The insertion phenomenon is based on two main potential factors: crystallographic and dynamic. The first is a set of non-occupied sites ranged in a manner which allows H^+/e^- to penetrate continuously and diffuse conveniently in the crystalline network. This latter contains a beneficial initial (H^+ , e^-) concentration. The second is the difference V_d between the two self velocities of H^+ and e^- . In fact, one of the two particles moves very slowly and is driven by the (relatively) very fast motion of the other. This drive is created by the internal electric field which imposes a common mean velocity to the inserted particles. The magnitude of V_d is maximal (maximum 1) at the beginning of the insertion (or FDS); it decreases significantly before reaching a zero value (corresponding to a common self velocities value) at $r \approx 0.50$. In the second half of the total reduction (TDS), the drive motion and roles switch over at the same time

with E_d . This step begins with a V_d null but it finishes by a second maximal value of $|V_d|$. Because of the self velocity weakness and the E_d action, the trapping is engaged and a continual slowness of the particles motion will be imposed. To sum up, the situations on TDS and FDS are practically and curiously symmetrical with respect to the point “ $r \approx 0.50$ ”.

Conclusion

This approach of extending the understanding of semiconductor theory to that of the reduction properties of γ -MnO₂ is a new finding. Based essentially on the differences between the values of the physical quantities [governing the (H⁺, e⁻) insertion in the dioxide], the above theory gives some results of great interest and clarifies several obscure points in the interpretation of the γ -MnO₂ characteristics. In fact, it:

1. Confirms that the author's published orders of magnitude on the values of D_{H^+} and S_r are correct.
2. Attributes the behaviour change at $r \approx 0.50$ to the orientation switching over of the Nernst field, after taking its null value.
3. Permits us to understand the dynamics of the insertion and relates it to equilibrium thermodynamics.
4. Points out the fundamental roles of the structure, initial (H⁺, e⁻) concentration and internal electric field (multiple roles).

In addition, this dynamic model constitutes, in a way, an ordinal programming as a function of r of the (H⁺, e⁻) insertion dynamics in γ -MnO₂.

Another matter of interest of this introduction to the dynamic theory of γ -MnO₂ is the fact that it can give answers to some problems concerning the behaviour of:

1. Several varieties of the manganese dioxide and electrode materials which reduce in a homogeneous phase by insertion of H⁺ (or Li⁺) and e⁻, (H. Kahil, unpublished)
2. Other categories of materials submitted to ambipolar diffusion.

In fact, the common fundamental factor governing the above behaviour is the internal electric field.

Finally, this series of articles [1, 2, 28] constitutes a new method for studying electrochemical systems with electron and proton (or Li⁺) insertion.

Appendix

Approximate determination of the mean diffusivities and ordinal intervals

Consider, as a first approximation, that:

1. The dynamic roles of the diffusion and conductivity tensors can be represented by the mean values \underline{D} and

$\underline{\sigma}$ which are accessible to the experimental measurements. Such a consideration allows the exploitation of the literature data concerning these two physical quantities published by Xia et al. [4, 23] and Kahil et al. [24].

2. All the inserted particles are still mobile or not trapped up to $r \approx 0.50$ (see first section of main text) and participate in the electric conduction. Thus, the concentration C can be estimated proportionally to its initial value C° (at $r^\circ = 0.08$) by the following formula:

$$C = C^\circ r / r^\circ \quad (\text{A1})$$

with, $C^\circ \approx 4 \times 10^{-3}$ mol/cm³ [2]. In the second half of the total reduction ($r > 0.50$), a part (P) of the mobile particles is trapped and Eq. (A1) becomes very approximative (but it continues to give useful order of magnitude).

Write now that the total conductivity measured by Xia et al. [4] is the sum of the electronic and protonic components:

$$\underline{\sigma} = \underline{\sigma}_{e^-} + \underline{\sigma}_{H^+} \quad (\text{A2})$$

Because we do not know the electronic and protonic values of the transfer numbers (nor their evolution as a function of r), it is not possible to calculate the partial values $\underline{\sigma}_{e^-}$ and $\underline{\sigma}_{H^+}$ nor \underline{D}_{e^-} and \underline{D}_{H^+} . Nevertheless, this difficulty is surmounted as follows. Firstly, using the Nernst–Einstein relation [39, 42] one can write

$$\underline{\sigma}_{e^-} = \underline{D}_{e^-} CF / RT$$

and

$$\underline{\sigma}_{H^+} = \underline{D}_{H^+} CF / RT \quad (\text{A3})$$

Equations (A3) indicate that diffusivity and conductivity engage the same concentration C . Write Eq. (A2) again as

$$\underline{\sigma} = (\underline{D}_{e^-} + \underline{D}_{H^+}) CF / RT$$

and put

$$\underline{D} = \underline{D}_{e^-} + \underline{D}_{H^+} \quad (\text{A4})$$

Then Eq. (A2) becomes

$$\underline{\sigma} = \underline{D} CF / RT \quad (\text{A5})$$

Now using the measured values of $\underline{\sigma}$, published by Xia et al. [4, 23] and the above formulae one can calculate \underline{D} as a function of r . Table 2 gives the results (at 298 K) corrected on the basis of Eq. (3) in the main text.

Secondly, the estimation of \underline{D}_{e^-} was obtained by the direct comparison between the values of \underline{D} and \underline{D}_{H^+} . This latter was determined using two coupled published data: NMR [24] and the rectified results of Xia et al. [23]. More precisely, the general shape of the Xia's published curve, which represents the variation of \underline{D}_{H^+} versus r , is adopted and corrected on the basis of Eq. (3)

Table 1 Numerical values for some quantities of interest in the first half of the total γ -MnO₂ reduction problem^a

	r						
	0.08	0.20	0.28	0.35	0.40	0.43	0.50
$\Delta\varepsilon$ (V) ^b	0.125	0.071	0.048	0.032	0.021	0.014	0
$(RT/F) \ln(\underline{D}_{e^-}/\underline{D}_{H^+})^{1/2}$ (v)	0.092	0.080	0.072	0.060	0.040	0.028	0

^aAt $T = 298$ K

^bSee Eq. (5)

of the main text. However, it has been shown (see earlier) that the order of magnitude of \underline{D}_{H^+} must be $\approx 10^{-9}$ cm²/s (in other words, the reactive surface of the γ -MnO₂ grain must be approximated by its geometrical surface instead of the BET one [2, 24, 51]). Therefore, by taking $\underline{D}_{H^+} \approx 0.6 \times 10^{-9}$ cm²/s at $r \approx 0.08$, all the other plotted values of the Xia's published curve are then rectified. The results obtained are collected in Table 2, which permits us to deduce that \underline{D}_{e^-} and \underline{D}_{H^+} have the same order of magnitude towards $r \approx 0.50$, and define, as shown in Table 3, the approximative ordinal intervals. The second part of Table 3 was estimated (or extrapolated) from the data of the same references [4, 23, 24]. In fact, whereas the values of $\underline{\sigma}$ or \underline{D} or \underline{D}_{e^-} continue to decrease for several orders of magnitude when r tends to 1, the \underline{D}_{H^+} value decreases very slowly and still has the

same order of magnitude. Notice that the behaviour change at $r \approx 0.60$ was confirmed by the dynamic results in the literature [14].

Finally, it is important to exploit the Table 2 data – FDS – to obtain (as a function of r) the empirical laws of variations of \underline{D}_{e^-} and \underline{D}_{H^+} . In fact, a simple look at the curves obtained by Xi et al. permits us to deduce that they can be (approximately) assimilated to straight line segments. For \underline{D}_{e^-} , two equations can be determined respectively for the intervals $0.08 \leq r \leq 0.28$ and $0.28 \leq r \leq 0.45$:

$$\ln \underline{D}_{e^-} = -9r - 13.7 \quad (\text{A6})$$

$$\ln \underline{D}_{e^-} = -33.3r - 7 \quad (\text{A7})$$

For \underline{D}_{H^+} , only one equation corresponding to $0.08 \leq r \leq 0.45$ is defined:

$$\ln \underline{D}_{H^+} = -0.97r - 21.1 \quad (\text{A8})$$

Table 2 Distributions of the total conductivity ($\underline{\sigma}$) and mean diffusivities (\underline{D} , \underline{D}_{e^-} , \underline{D}_{H^+}) at various reduction degrees (r) of γ -MnO₂. Data shown are from published data on the dynamics of the (H⁺, e⁻) insertion in γ -MnO₂ [4, 23, 24]^a

	r						
	0.08	0.25	0.28	0.35	0.40	0.45	0.47
$10^3 C^b$	4	12.5	14	17.5	20	22.5	23.5
$10^3 \underline{\sigma}^c$	8	5.5	4.3	0.7	0.15	0.06	0.025
$10^9 \underline{D}^d$	540	118	83	11	2	0.7	0.3
$10^9 \underline{D}_{H^+}^e$	0.6	0.51	0.50	0.47	0.44	0.42	0.34
$10^9 \underline{D}_{e^-}^f$	539.4	117.5	82.5	10.5	1.5	0.3	0.0 <i>n</i>

^aAt $T = 298$ K. n is an arbitrary integer; $\underline{\sigma}$ in Ω^{-1} cm⁻¹, \underline{D} in cm²/s

^bComputed from Eq. (A1)

^cPublished by Xia et al. [4, 23] and corrected on the basis of Eq. (3) in the main text

^dComputed from Eq. (A5) and corrected on the basis of Eq. (3) in the main text

^eDetermined using published data: NMR [24] and the rectified results of Xia et al. [4, 23]

^fEstimated by simple subtraction between the values of \underline{D} and \underline{D}_{H^+}

Table 3 Decreasing of $\underline{D}_{e^-}/\underline{D}_{H^+}$ during the total reduction of γ -MnO₂. The values of \underline{D}_{e^-} and \underline{D}_{H^+} are estimated from the data of Table 2

FDS			
r	$0.08 \leq r \leq 0.28$	$0.28 \leq r \leq 0.45$	$0.45 \leq r \leq 0.50$
$\underline{D}_{e^-}/\underline{D}_{H^+}$	$\gg 1$	> 1	≥ 1
TDS			
r	$0.50 \leq r \leq 0.60$	$0.60 \leq r \leq 1$	
$\underline{D}_{e^-}/\underline{D}_{H^+}$	≤ 1	$\ll 1$	

References

- Kahil H (1996) Ionics 2: 361
- Kahil H (1995) J Phys Condens Matter 7: 3227
- Preisler E (1975) J Appl Electrochem 6: 311
- Xia X, Hong L, Zhen-Hai C (1989) J Electrochem Soc 136: 266
- Ruetschi P, Giovanoli R (1984) J Electrochem Soc 131: 2737
- Ouboumour H, Cachet C, Bodé M, Yu LT (1995) J Electrochem Soc 142: 1061
- Mondolini C, Laborde M, Rioux J, Anoni E, Clément C (1992) J Electrochem Soc 139: 954
- Kordesch K, Gsellmann J, Peri M, Tomantschger K, Chemelli R (1981) Electrochim Acta 26: 1495
- Harer W, Kordesch K (1985) In: The 2nd battery material symposium, Graz, Austria, vol 2, p 231
- Tye FL, Tye SW (1995) J Appl Electrochem 25: 425
- Fillaux F, Ouboumour H, Tomkinson J, Yu LT (1991) Chem Phys 149: 459
- Fillaux F, Ouboumour H, Cachet C, Tomkinson J, Kearley GJ, Yu LT (1992) Chem Phys 164: 311
- Fillaux F, Ouboumour H, Cachet C, Tomkinson J, Clément C, Yu LT (1992) Physica B 180: 680
- Fillaux F, Ouboumour H, Cachet C, Tomkinson J, Clément C, Yu LT (1993) J Electrochem Soc 140: 592
- Tye FL (1992) In: Swinkels DAJ (ed) Progress in batteries and battery materials (IBA meeting, Sydney) vol 11. ITE-JEC
- Maskell WC, Shaw JEA, Tye FL (1981) Electrochim Acta 26: 1403
- Maskell WC, Shaw JEA, Tye FL (1982) J Appl Electrochem 12: 101
- Ohzuku T, Kitagawa M, Hirai T (1989) J Electrochem Soc 136: 3169
- Ohzuku T, Kitagawa M, Hirai T (1990) J Electrochem Soc 137: 40

20. Ohzuku T, Kitagawa M, Hirai T (1990) *J Electrochem Soc* 137: 769
21. Ohzuku T, Kato J, Sawai K, Hirai T (1991) *J Electrochem Soc* 138: 2556
22. Atlung S (1975) In: Manganese dioxide symposium. I C Sample Office, Cleveland, p 47
23. Xia X, Hong L, Zhen-Hai C (1989) *J Electrochem Soc* 136: 2771
24. Kahil H, Dalard F, Guitton J, Cohen Addad JP (1982) *J Surf Technol* 16: 331
25. Fitzpatrick J, Tye FL (1991) *J Appl Electrochem* 21: 130
26. Tye FL (1976) *Electrochim Acta* 30: 415
27. Maskell WC, Shaw JEA, Tye FL (1982) *J Power Sources* 8: 113
28. Kahil H (1999) In: 12th IBA Annecy-Grenoble Meeting, ITE Battery Letters 1: 55
29. Barnard R, Randell CF, Tye FL (1980) *J Appl Electrochem* 10: 127
30. Boltaks H (1977) Diffusion et défauts ponctuels dans les semi-conducteurs. Mir, Moscow
31. Reiss H (1953) *J Chem Phys* 21: 1209
32. Reiss H, Fuller CS (1956) *J Metals* 12: 276
33. Reiss H, Fuller CS, Morin FJ (1956) *Bell Syst J* 35: 535
34. Fer F (1970) Thermodynamique macroscopique. Gordon and Breach, Paris
35. Martinet J (1990) Thermocinétique approfondie. Lavoisier, Paris
36. Carslaw HS, Jaeger JC (1990) Conduction of heat in Solids. Clarendon Press, Oxford
37. Chabre Y, Pannetier J (1995) *Prog Solid State Chem* 23: 1
38. Wruck WJ, Reichman B, Bullock KR, Kao W (1991) *J Electrochem Soc* 12: 3560
39. Philibert J (1985) La diffusion dans les solides. Presses Universitaires de France, Paris
40. Garrels RM, Christ CL (1967) Equilibre des minéraux et de leurs solutions aqueuses. Gauthier-Villars, Paris
41. Manning JR (1968) Diffusion kinetics for atoms in crystals. Van Nostrand, Princeton, NJ
42. Wepper W (1990) Solid state microbatteries. Plenum, New York
43. Schmalzried H (1995) Chemical kinetics of solids. VCH, Weinheim
44. Antoncik E (1995) *J Electrochem Soc* 142: 3170
45. Calot G (1965) Cours de statistique descriptive. Dunod, Paris
46. Scott AB (1960) *J Electrochem Soc* 107: 941
47. Kornfeil F (1962) *J Electrochem Soc* 109: 349
48. Huber R, Bauer J (1967) *J Electrochem Tech* 5: 542
49. Malati MA, Rophail MW, Bhayat II (1981) *Electrochim Acta* 26: 239
50. Anderson TN (1992) In: Swinkels DAJ (ed) Progress in batteries and battery materials (IBA Meeting, Sydney), vol 11. ITE-JEC
51. Kahil H (1985) Etat thesis, INP Grenoble